Particle Deposition in Porous Geothermal Reservoir

Haiyan Lei[1,2], Jing Cui,[1,2], Chuanshan Dai[1,2]*, Likun Dong

[1] Key Laboratory of Efficient Utilization of Low and Medium Grade Energy, MOE, Tianjin University, China
[2] School of Mechanical Engineering, Tianjin University, Tianjin 300350, China

Keywords

Micro Particles, porous reservoir, deposition, temperature gradient

ABSTRACT

The clogging of the micro particles at the interfaces of porous geothermal reservoir during reinjection is a long-standing bottleneck in geothermal utilization. This paper numerically simulated the effects of particle density, particle concentration, the ratio of particle size and porous media pore size, on the particle migration at the fluid-porous media interface. The Lattice-Boltzmann method (LBM) that is easy to deal with complex boundaries is used to simulate the fluid flow. By Newton's law to deal with the particle movement, can solve the influence of particle size, geometry and deposition morphology on particle interaction, which is difficult to solve for the previous numerical simulation. The conclusions are: (1) The amount of particle deposition both at the interface and inside the porous media increases as particle density increase. The greater the particle density, the earlier the particle clogging occurs at the interface. (2) The particle concentration has no significant effect on the amount of particle deposition at the interface, but affects the clogging time at the interface.

1. Introduction

Deposition and clogging of micro particles is common during geothermal sandstone reinjection. Liu (2016) indicated that in Beijing in 1981, there were 64 reinjection systems. However, only 13 systems were in operation by 1991, and the rest were stopped due to the clogging. Lindesy (1992). indicated that in 1986 Maryland's 207 reinjection systems, 33% stopped operating due to the clogging within two years, and by 1990, the number of outage systems rose to 50%. In this paper, particle migration in porous geothermal reservoir is simulated using lattice Boltzmann method (LBM). The single particle deposition and the collision of two particles were respectively simulated. By comparing the moving speed and trajectory of the particles under the same condition with previous study, the accuracy of the solid-liquid interface treatment methods, the particle motion treatment methods and the calculation method of the collision force between particles were validated. Based on this, the deposition of multiple particles in porous media was further studied.

2. Numerical Methods

2.1 D2Q9 model

A complete lattice Boltzmann model usually consists of three parts: the discrete velocity model, the equilibrium state distribution function, and the evolution equation of the distribution function. D2Q9 model (Qian *et al.*, 1992) was used here to simulate the particle deposition, the evolution equation of single relaxation model is:

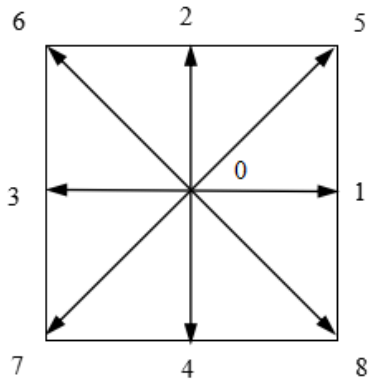

Figure 1: D2Q9 model of speed diagram

The speed vector corresponding to this model is defined as

$$e_i = \begin{cases} 0 & i = 0 \\ c * \left[cos\left(\frac{(i-1)\pi}{2}\right), sin\left(\frac{(i-1)\pi}{2}\right)\right] & i = 1,2,3,4 \\ c * \left[cos\left(\sum_5^i((i-5)\pi)\right), sin\left(\sum_5^i\left(\frac{\pi}{2}+(i-5)\pi\right)\right)\right] & i = 5,6,7,8 \end{cases} \quad (1)$$

where *i* denotes the speed direction, $c = \delta x/\delta t$, δx and δt are the corresponding grid and time step, respectively. For a uniform grid, $\delta x = \delta t$.

The single relaxation model evolution equation with volumetric force terms is:

$$f_i(x + \vec{e_i}\Delta t, t + \Delta t) = f_i(\vec{x}, t) - \frac{1}{\tau_f}\left[f_i(\vec{x}, t) - f_i^{eq}(\vec{x}, t)\right] + (1 - \frac{1}{2\tau})F_i\Delta t \quad (2)$$

where $f_i(\vec{x}, t)$ is the density distribution function corresponding to the discrete velocity $\boldsymbol{e_i}$, τ_f is dimensionless relaxation time. The equilibrium distribution function f_i^{eq} take the form:

$$f_i^{(eq)} = \omega_i\rho\left[1 + \frac{3}{c^2}(\vec{e_i}\cdot\vec{u}) + \frac{4.5}{c^2}(\vec{e_i}\cdot\vec{u})^2 - \frac{1.5}{c^2}u^2\right] \quad (3)$$

where ω_i, ρ, $\vec{u}$, and c are weighting coefficient, fluid density and the velocity vector, respectively.

The velocity vector and the density of fluid are obtained by

$$\rho\vec{u} = \sum_i \vec{e_i}\cdot f_i + \frac{\Delta t}{2}\vec{F}; \qquad \rho = \sum_i f_i \quad (4)$$

The kinematic viscosity of the fluid is defined as follows:

$$\nu = \frac{1}{3}(\tau - \frac{1}{2})c^2\Delta t \quad (5)$$

2.2 Immersed Boundary-LBM

Immersed Boundary-LBM 0 is used to deal with solid-liquid two-phase problem and complex boundary conditions. The density distribution function $f_i^*(\vec{x}, t + \Delta t)$ at time $t + \Delta t$ is given by

Equation (2), and then $\rho(\vec{x}, t+\Delta t)$ is given by Equation (4). $\overrightarrow{U_P}(\vec{x}, t+\Delta t)$ is particle velocity at $\vec{x}$, thus the equilibrium density distribution function is:

$$f_i^{(eq,*)}(\vec{x}, t+\Delta t) = \omega_i \left[\rho(\vec{x}, t) + \rho_0 \left(\frac{3}{c^2}\left(\vec{e_i} \cdot \overrightarrow{U_P}(\vec{x}, t+\Delta t)\right) + \frac{4.5}{c^2}\left(\vec{e_i} \cdot \overrightarrow{U_P}(\vec{x}, t+\Delta t)\right)^2 - \frac{1.5}{c^2}\overrightarrow{U_P}(\vec{x}, t+\Delta t)^2\right)\right] \quad (6)$$

The density distribution function at time $t+\Delta t$ is further modified to

$$f_i(\vec{x}, t+\Delta t) = \left(1-\varphi_B(\vec{x})\right) f_i^*(\vec{x}, t+\Delta t) + \varphi_B(\vec{x}) f_i^{(eq,*)}(\vec{x}, t+\Delta t) \quad (7)$$

According to Newton's law of motion, the motion of suspended particles in a fluid can be expressed as:

$$M_s \frac{d\overrightarrow{U_c}}{dt} = -\int \vec{F}^{IB} dV + \frac{\partial}{\partial t}\int \rho_f \vec{u} dV + \left(1-\frac{\rho_f}{\rho_s}\right) M_s \vec{g} + \vec{F}^{col} + \vec{F}^{w} \quad (8)$$

where M_s is the mass of the particles, $\overrightarrow{U_c}$ is the average speed of the particles, $\vec{F}^{IB}$ is the direct force added to each lattice point. This paper uses Equation (9) (Fadlun et al., 2000) to calculate the collision force between particles:

$$\vec{F}_{ij}^{col} = \begin{cases} 0 & \left\|\vec{x}_i - \vec{x}_j\right\| > R_i + R_j + \sigma \\ \frac{C_{ij}}{\varepsilon_p}\left(\frac{\left\|\vec{x}_i - \vec{x}_j\right\| - (R_i + R_j + \sigma)}{\sigma}\right)\left(\frac{\vec{x}_i - \vec{x}_j}{\left\|\vec{x}_i - \vec{x}_j\right\|}\right) & \left\|\vec{x}_i - \vec{x}_j\right\| \le R_i + R_j + \sigma \end{cases} \quad (9)$$

where $\vec{x}_i$ and $\vec{x}_j$ are the center of particles i and j, R_i and R_j are the radius of particles i and j, C_{ij} is the standard force, which is buoyancy force in this paper, ε_p is the stiffness coefficient of the collision particles. σ is the safety distance. The calculation of collision force $\vec{F}^{w}$ between the particle and the wall is similar to $\vec{F}^{col}$. The motion of suspended particles has rotation in addition to translation, according to the Newton angular momentum theorem:

$$I_s \frac{d\omega_c}{dt} = -\int \left(\vec{x}_b - \vec{X}_c\right) \vec{F}^{IB} dV + I_f \frac{d\omega_c}{dt} \quad (10)$$

where I_s and I_f are the moment of inertia of the particles and the fluid, ω_c is the particle angular velocity, $\vec{X}_c$ is the center of the particles. The particle center position and particle velocity at time n+1 can be calculated by Eqs.(8) and (10).

2.3 Program verification

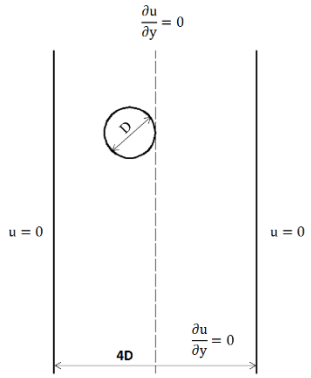

Figure 2: Biased single particle deposition

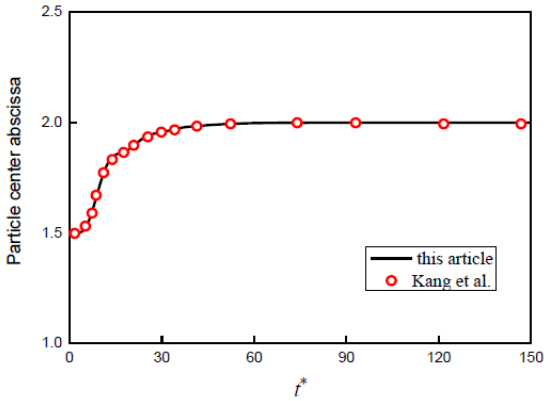

Figure 3: Particle circle abscissa changes over time

As shown in Fig. 2, a particle of diameter D is placed in the fluid, the abscissa of the initial position deviates from the center line D/2, the particle density ρ=1.00232, and the initial velocity is v=0. The relaxation time τ = 0.65, which is the same as Kang et al. (2011).

In order to calculate the gravitational acceleration in LBM, the reference Reynolds number is used in this paper, which is defined as:

$$\mathrm{Re}_{ref} = U_{ref} D/\nu; \quad U_{ref} = \sqrt{\pi\ (\mathrm{D}/2)\ (\rho_r - 1)\mathrm{g}} \tag{11}$$

Re_{ref}=40.5, the calculation area is 4D×160D, the initial state of the fluid is stationary, the left and right walls of the channel are set as fixed no-slip boundary conditions, and the upper and lower boundary conditions are infinite. Table 1 is a comparison with previous calculations.

Table 1: Reynolds number comparison

	This article	Gan *et al.*	Kang *et al.*
Re_T	20.7	21.0	21.2

As can be seen from Fig. 3, the particles gradually move towards the center of the flow channel and stabilize there, which is in good agreement with the results of Kang (2011), indicating the correctness of program.

3. Simulation of particle Deposition in Porous Media

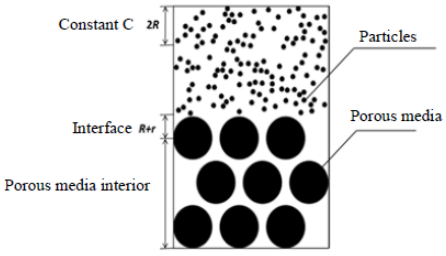

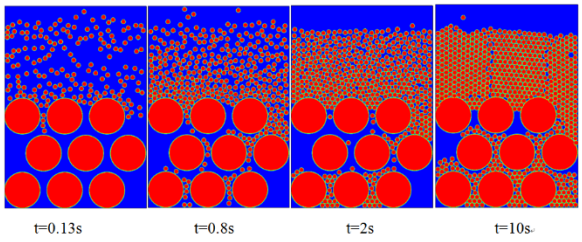

Figure 4: The particle deposition in porous media **Figure 5: Particle deposition**

As shown in Figure 4 shows that micro particles are randomly distributed in the porous media. The diameter of the porous media D_P=800 μm, the particle size of the suspended particles dp=100 μm, the dynamic viscosity $\mu = 1 \times 10^{-3}$ m^2/s, and the density$\rho = 1$ g/cm^3. The initial velocity of particles and fluid is 0. The concentration of particles in the upper 3.7 mm-4.5 mm area is kept constant during particle deposition. When particles move out of the area, a

corresponding number of particles will be automatically generated to ensure the concentration of particles in this area.

3.1 Effect of Particle Density on Deposition Characteristics

Figure 5 shows the particle deposition process with $\rho = 2.45\text{g}/\,cm^3$ $c = 18.5$ 个$/mm^2$. It can be seen that the particles first deposit on the surface of the porous medium and then gradually move through the interface to the inside of the porous medium. The time and the amount of deposition are dimensionless, that is,

$$t^*=t\,\mu\,/(\,\rho D_P 2),\quad m^*=m/m_1 \tag{12}$$

where, t^* and m^* are the dimensionless time and deposition amount, t is the real time, m is the deposition amount, and m_1 is the reference deposition amount.

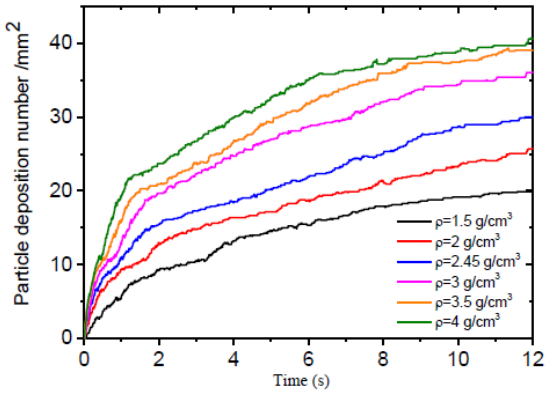

Figure 6: Total particle deposition changes over time at different densities

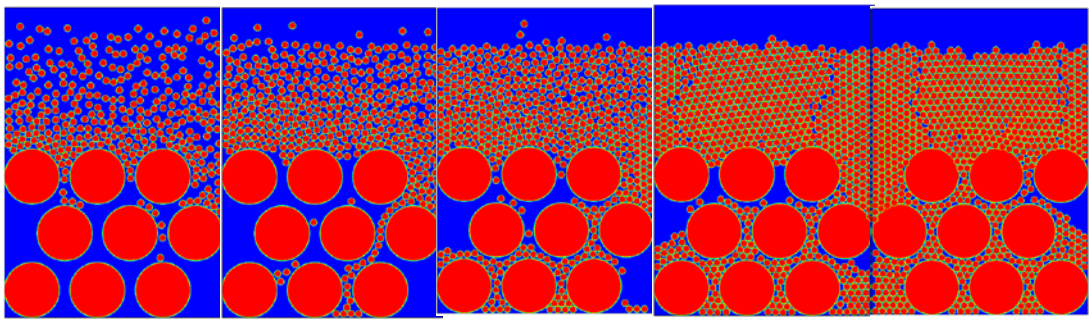

Figure 7: Total particle deposition changes over time (ρ = 3.5 g/cm^3)

As can be seen from Figures 6 and 7, total deposition amount of particles increases with time and particle density, and the particle deposition rate gradually decreases with time. The particle deposition rate has a more obvious turning point. The greater the particle density, the earlier the turning point of the deposition rate appears. The reason may be that when the number of particles

at the interface reaches a certain amount, the clogging at the interface makes it difficult for the particles to migrate to the inside of the porous media; and the greater the particle density, the easier it will accumulate at the interface and the earlier the clogging time will occur.

3.1 Effect of Particle Concentration on Particle Deposition

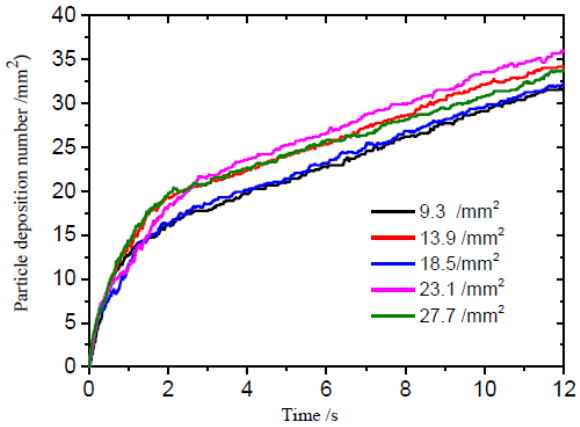

Figure 8: The change of particle deposition with time under different concentration

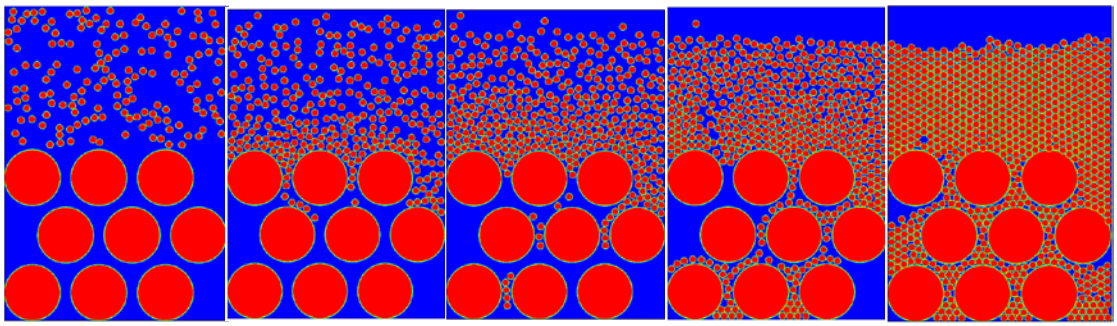

Figure 9：Particle deposition

Figures 8 and 9 show the total particle deposition change over time. It can be seen that the curve changes linearly after *t*=2, and the deposition rate is almost the same at different concentrations, the reason for the difference in the deposition amount is mainly the clogging time.

4. Conclusions

In this paper, the effect of the particle density and concentration on its deposition at the interface of porous media was simulated by LBM based on program validation, and the conclusions were obtained: (1) The deposition amount of particles in porous media increases with the increase of particle density. The larger the particle density, the earlier the particle clogging occurs at the porous media interface. (2) The particle concentration has no significant effect on the deposition amount of particle at the interface, but affects the time of clogging at the interface.

ACKNOWLEDGEMENTS

This work is financially supported by the National Science Foundation of China (Grant No. 41672234 and 41574176) and International Clean Energy Talent Programme (iCET) of China Scholarship Council.

REFERENCES

Liu, Q, Cui, X, and Zhang, C, et al. "Experimental investigation of suspended particles transport through porous media: particle and grain size effect". Environmental Technology, 37(2016), 854.

Lindsey, G, Roberts, L, and Page, W. "Inspection and maintenance of infiltration facilities". Research Policy, 47(1992), 481-486.

Qian,Y.H., D'Humières, D., and Lallemand, P. "Lattice BGK models for Navier-Stokes equation". Europhysics Letters, 17(1992), 479.

Lin, S.Y., Lin, C.T., Chin, Y.H., et al. "A direct‐forcing pressure‐based lattice Boltzmann method for solving fluid–particle interaction problems". International Journal for Numerical Methods in Fluids, 66(2011), 648-670.

Fadlun, E., Verizicco, R., Orlandi, P., et al. "Combined immersed-boundary finite-difference methods for three-dimensional complex flow simulations". Journal of Computational Physics, 16(2000), 35-60.

Kang, S.K., Hassan, Y.A. "A direct-forcing immersed boundary method for the thermal lattice Boltzmann method". Computers & Fluids, 49(2011), 36-45.

Gan, H., Chan,g J., and Feng, J.J., et al. "Direct numerical simulation of the sedimentation of solid particles with thermal convection". Journal of Fluid Mechanics, 481(2003), 385-411.